 doi:10.20944/preprints201802.0032.v1

*Article*

# An inverse aeroacoustic problem with aerodynamic constraint for a helicopter rotor

**Qinghe Zhao [1], Xiaodong Li [2,*]**

[1] School of Energy and Power Engineering, Beihang University, Beijing 100191, China; zhaoqinghe2001@163.com
[2] School of Energy and Power Engineering, Beihang University, Beijing 100191, China;
* Correspondence: lixd@buaa.edu.cn; Tel.: +86-010-82338579

Received: date; Accepted: date; Published: date

**Abstract:** An inverse aeroacoustic problem for a helicopter rotor combined with aerodynamic constraint is proposed based on Ffowcs Williams and Hawkings equation in subsonic. The rotor noise includes thickness noise and loading noise when quadrupole noise is neglected. Thickness noise is related to geometry and motion conditions. Loading noise is related to the pressure on the wall. Therefore, the equation between pressure on the wall and far-field noise can be established, thus the pressure on the wall can be obtained by solving this equation. Since this equation is an ill-posed, the singular value decomposition combined with the regulation method is applied and the aerodynamic constraint is taken into account. The direct noise prediction is verify firstly and then the inverse problem is solved. The reconstruction pressure is compared to the input data. The result is in good agreement with the input value. At the same time, the influence of interference noise is also considered. Under low signal-to-noise ratio, the reconstruction result is also reasonable.

**Keywords:** inverse acoustic problem; helicopter rotor; Ffowcs Williams and Hawkings equation; aerodynamic constraint; Thikhonov method

## 1. Introduction

High speed rotating blades have many applications in industry, including rotor, propeller, compressor, and turbine et al[1-5]. This kind of rotating blade has a high speed in the tip region, its loading is larger but its thickness is thinner. The traditional measurement method includes embedded pressure sensor or open pressure hole. The embedded pressure sensor method requires higher installation accuracy of the test instrument. This can produce a large error especially in high-speed rotation. The rotor interior space is limited; it is difficult to install sensors. The open pressure hole is also a traditional measurement method, it is also difficult to arrange the plastic tube. Non-contact measurement technology can overcome these limitations, especially suitable for the tip region of rotor.

There have been many advances on the inverse aeroacoustic problem during past two decades. For example, Li and Zhou[6] proposed an inverse model for the reconstruction of steady pressure distribution on propeller based on three-dimension Ffowcs Williams and Hawkings (FW-H) equation. Grace and Atassi[7-8] solved an inverse aeroacoustic problem associated with a flat-plate airfoil in unsteady compressible flow. They also tested the sensitivity to errors in both the far-field input data and the mean-flow input parameters. The results of the sensitivity analysis for the input data show that the magnification of input error due to ill-posed can be controlled by optimal choices of the regularization parameter and the measurement locations. Nelson and Yoon [9] examined the conditioning of this inverse problem, particularly with regard to the geometry and number of sources and measurement positions and the non-dimensional frequency. Wood and Grace[10] developed an optimally determining the near-field pressure method without relying on a user-specified regularization parameter. Yu and Zhuang[11] developed an acoustic intensity-based

Preprints (www.preprints.org) | NOT PEER-REVIEWED | Posted: 5 February 2018 doi:10.20944/preprints201802.0032.v1

inverse method for predicting the radiated field of a stationary sound source, the method is more stable and the acoustic reconstruction is less dependable on the locations of the input. Trabelsi et al[12] investigated an inverse method to evaluate the unsteady rotating forces acting on the fluid by the fan's blade. The reconstruction reveals the conditioning of the inverse problem depends on the aeroacoustic source and the sensors number as well as on the studied frequency. Zhang et al[13] also proposed a time-domain inverse technique for the localization and quantification of rotating sound sources, the results was more accurate compared with the time-domain rotating beamforming. Madoliat et al[14] studied the acoustic model order reduction for the lowest condition number in inverse method.

Thickness noise is related to geometry and motion conditions. Loading noise is related to the pressure on the wall. Therefore, the relationship between pressure on the wall and far-field noise can be established, thus the pressure on the wall can be obtained by solving this equation. The basic aim of this paper is to reconstruct the pressure distribution on the rotor by using acoustic signals. The difficulty of solving the inverse problem is the equation is ill-posed. The singular value decomposition method combined with the regulation method is applied and the aerodynamic constraint is taken into account. The structure of the paper is as follows. Section 2 presents mathematical formulation. Section 3 gives the numerical results. Some conclusions are finally drawn in Section 4.

## 2. Mathematical Formulation

Helicopter radiation noise can be divided into three categories noise, thickness noise, loading noise and quadrupole noise[18]. The thickness noise is generated by the displacement of fluid as the blade rotates. The loading noise is generated by distributed aerodynamic forces on the blade surface. The quadrupole noise is only important when the rotor tip Mach number is transonic or supersonic and so can be neglected for a subsonic moving surface. So in this paper only the thickness noise and loading noise of the FW-H equation are utilized.

$$\Box^2 p' = \frac{\partial}{\partial t}[\rho_0 v_n |\nabla f| \delta(f)] - \frac{\partial}{\partial x_i}[l_i |\nabla f| \delta(f)] \tag{1}$$

Farassat[19-21] had given several integral solutions to Eq.(1), the equation is as follows

$$p'(\bar{x},t) = p'_L(\bar{x},t) + p'_T(\bar{x},t) \tag{2}$$

The thickness noise is the sum of term (3) and term (4)

$$a_1 = \int_{f=0} \frac{\rho_0 \dot{U}_n}{r(1-M_{ar})^2} dS \tag{3}$$

$$a_2 = \int_{f=0} \frac{\rho_0 U_n (r \cdot \dot{M}_{ar} \cdot \hat{r}_i + c_0 (M_{ar} - M_a^2))}{r^2 (1-M_{ar})^3} dS \tag{4}$$

The loading noise is the sum of term (5), term (6) and term (7)

$$a_3 = \frac{1}{c_0} \int_{f=0} \frac{\dot{l}_i \cdot \hat{r}_i}{r(1-M_{ar})^2} dS \tag{5}$$

$$a_4 = \int_{f=0} \frac{l_r - l_i \cdot M_{ai}}{r^2 (1-M_{ar})^2} dS \tag{6}$$

$$a_5 = \frac{1}{c_0} \int_{f=0} \frac{l_r (r \cdot \dot{M}_{ari} \cdot \hat{r}_i + c_0 (M_{ar} - M_a^2))}{r^2 (1-M_{ar})^3} dS \tag{7}$$

Preprints (www.preprints.org) | NOT PEER-REVIEWED | Posted: 5 February 2018 doi:10.20944/preprints201802.0032.v1

The thickness noise term is only related to the geometry and motion, so it can be predicted directly. Instead, the loading noise term is related to the pressure on the surface, which can be predicted when the pressure is known.

### 2.1. Solution of Matrix Equation

The noise items are rearranged, one term is related to geometry and motion, and another term is related to pressure on the wall. It can be written as Eq.(8)

$$[4\pi p^{'}] = [A][p] + [B][v_n] \tag{8}$$

Then, the relationship between pressure on the wall and far-field noise can be expressed as

$$[A][p] = [4\pi p^{'}] - [B][v_n] \tag{9}$$

The simplified form of this equation can be written as

$$Ax = b \tag{10}$$

Where $A$ is the model matrix with an over determined dimension, $x$ corresponds to the pressure on the wall, $b$ stands for the sound pressure of observing points after subtracting the thickness noise. Singular value decomposition (SVD) is used to decomposed the ill-posed matrix, which can be represented in the following form.

$$A = U\begin{bmatrix}\Sigma \\ 0\end{bmatrix}V^T \tag{11}$$

where $U = (u_1,...,u_m)$ and $V = (v_1,...,v_n)$ are matrices with orthogonal columns, $U^TU = I_m$, $V^TV = I_n$, $T$ denotes transposition. $\Sigma = diag[\sigma_1,...,\sigma_n]$ are singular values. The result of direct solution is

$$x = Vdiag(\frac{1}{\sigma_i})U^Tb \tag{12}$$

Generally, this kind of equation is ill-posed. The so-called ill-posed problem means that the existence, uniqueness or stability of the solution is not satisfied. The stability of the solution is not satisfied means that the small disturbance on the right side of the equation will lead to the infinite change of the solution. The general method for solving ill-posed problems is using the regularization method[15-17]. The Tikhonov regularization method is based on variation principle, which is widely used in all kinds of inverse problem research, and the solution of equation can be expressed as

$$\min(\|Ax - b\|_2 + \lambda\|Lx\|_2) \tag{13}$$

The regulation value $\lambda$ weights the solution norm and the residual norm, which can be chosen by L curve method.

$$x_{reg} = Vdiag(\frac{\sigma_i}{\sigma_i^2 + \lambda^2})U^Tb \tag{14}$$

### 2.2. Solution with Aeroacoustic Constraints

Generally, there is no exact solution to ill-posed equations. However, By using prior knowledge, the result of a close solution can be obtained. In this paper, the pressure on the wall is the variable. The variable need to comply with certain physical laws, which is also known as aerodynamic restraint. Figure 1 shows the aerodynamic constraint. The leading edge is the aerodynamic stagnation point, the pressure is the maximum. The flow velocity increases and

Preprints (www.preprints.org) | NOT PEER-REVIEWED | Posted: 5 February 2018 doi:10.20944/preprints201802.0032.v1

reaches the maximum speed and the pressure reached a minimum at the same time. Then the pressure increase to trailing edge gradually. The detailed content is given below

$$\begin{cases} p_i \le p_{i+1}, 0 \le x \le x_1 \\ p_j \ge p_{j+1}, x_2 \le x \le 1 \end{cases} \tag{15}$$

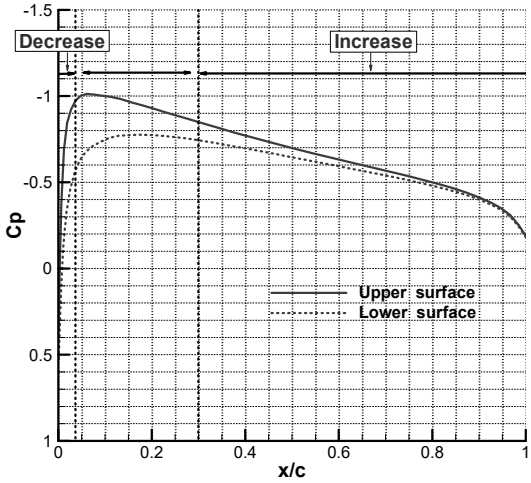


**Figure 1.** The pressure distribution on the rotor surface

## 3. Direct Problem Validation Case

Firstly, the accuracy of noise prediction method is verified based on the FW-H equation. A hovering rotor acoustic experiment was carried out at French-German Research Institute of Saint Louis in 1985[22-23]. The model is called ISL model. Its geometry information is given in Table 1.

**Table 1.** Rotor geometry parameters

| Parameter | Value |
|---|---|
| Rotor diameter | 2.00 m |
| Root radius | 0.28 m |
| Profile kind | NACA0012 |
| Profile chord | 110.15 m |
| Linear twist | 226.945 degree |
| Blade mass | 331.4 kg |
| Blade number | 2 |

The experiment environment is shown in Figure 2, which is cited from reference[23]. The rotor tip Mach number is 0.65 in this experiment. In Figure 2, M01 stands for the first microphone one span away from rotational axis in the rotation plane, M02 stands for the second microphone, which is 20 degrees below the first microphone. The time-domain signals obtained by the two microphones are used to verify the noise prediction method.

Preprints (www.preprints.org) | NOT PEER-REVIEWED | Posted: 5 February 2018 doi:10.20944/preprints201802.0032.v1

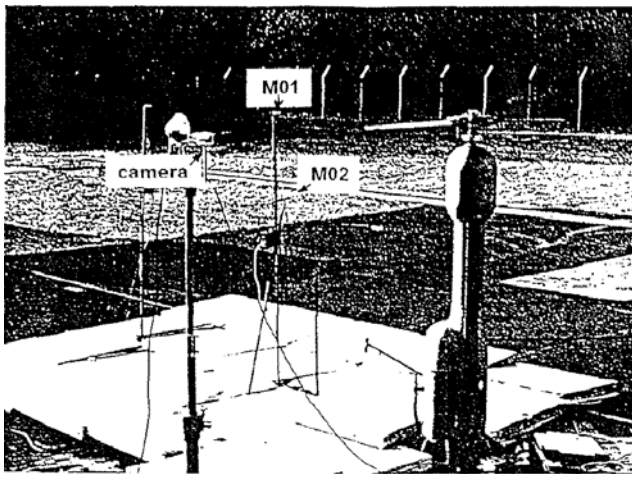


**Figure 2.** Aeroacoustic experiment of ISL rotor [23]

Noise prediction needs to base on pressure information on the wall, and the pressure on the wall is obtained by Computational Fluid Dynamics(CFD) simulation firstly. In hover case due to the symmetry of the flow in rotational coordinate system, the flow can be treated as a steady state. Once the pressure on the rotor is obtained, the radiation noise can be predicted. The Figure 3(a) is the comparison between the predicted result and the experimental data of M01 microphone, it can be seen that the two agree very well. The Figure 3(b) is the comparison between the predicted result and the experimental data of M02 microphone. M02 microphone measurement signal has some oscillations, and the agreement is quite well.

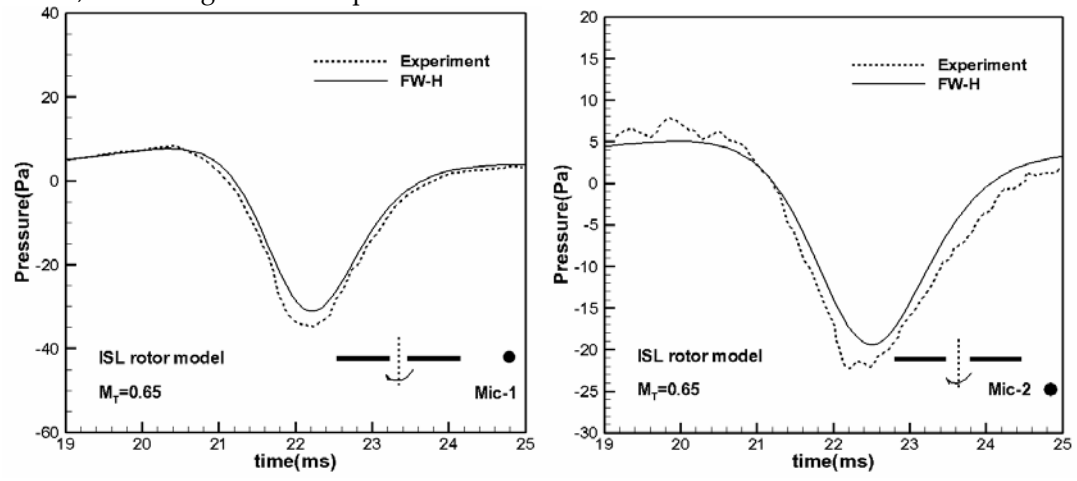


(**a**) (b)

**Figure 3.** Validation of sound prediction method

## 4. Inverse Problem Solutions

The difference from solving direct problem is that to solve the inverse problem, more microphones are generally needed. Therefore, a virtual experiment is carried out, and the diagram is shown in Figure 4. The rotor model is ISL rotor, which rotates in clockwise direction. The microphones are arranged in an array of 2 meters in diameter. The black circle on the left side represents the microphone. The microphone array center is 3 meters away from the rotational axis, which includes 35 microphones.

Preprints (www.preprints.org) | NOT PEER-REVIEWED | Posted: 5 February 2018 doi:10.20944/preprints201802.0032.v1

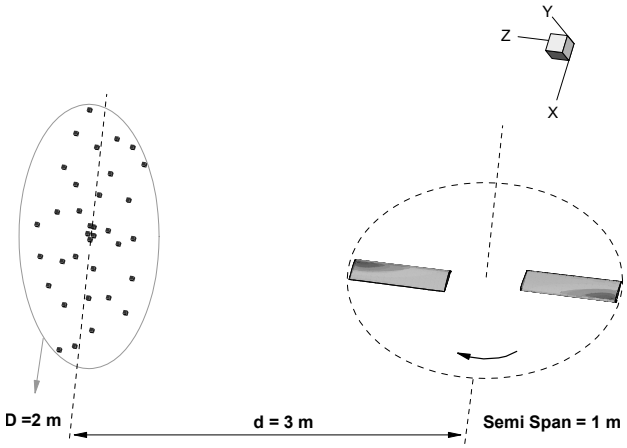


**Figure 4.** Test arrangement of rotor and microphones

A series of data collected through this virtual experiment is shown in Figure 5. The data on the same curve represents the experiment data obtained by same microphone at different times. The dashed line in the Figure 5 means the experimental data are obtained by different microphones at the same time. There are 35 microphones, each microphone obtain 180 experiment data within half period. The over-determined equation of $35\times180=6300$ is built. There are 400 grid element on the rotor surfaces, 40 grid in the chord direction and 10 grid in the span direction. So the $6300\times400$ coefficient matrix is built.

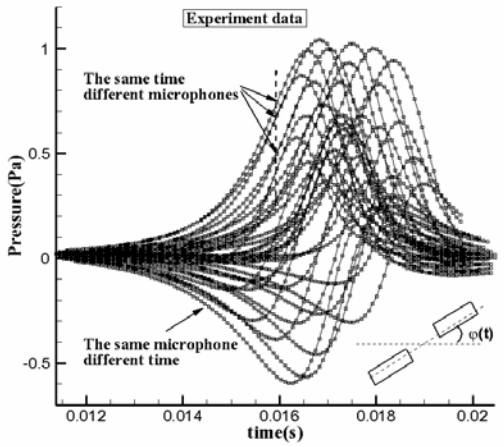


**Figure 5.** Time domain signals of different microphones

The process of solving the inverse problem is as follows:

- Thickness noise is obtained with known geometric information and motion condition;
- Loading noise is obtained by subtracting the thickness noise from the total noise;
- The over-determined equations between wall pressure and far-field noise are established;
- Regularization parameter is obtained by L curve method;
- To Solve the optimization problem with aerodynamic constraint.

### *4.1. Inverse problem case under ideal conditions*

First, the inverse problem under ideal condition is solved, which means that there is no interference noise. Figure 6 shows the pressure contour lines of the rotor surface with aerodynamic constraint is taken into account. The Figure 6(a) is the reconstructed contour lines of the upper surface and Figure 6(b) is the reconstructed contour lines of the lower surface. The solid line is the pressure obtained by the CFD simulation, and the term is also used as the source of noise radiation. The dashed line is the reconstructed pressure distribution. It can be seen that the reconstructed pressure distribution more accurately identifies the low pressure zone of the tip, and the result is more smoother.

Preprints (www.preprints.org) | NOT PEER-REVIEWED | Posted: 5 February 2018 doi:10.20944/preprints201802.0032.v1

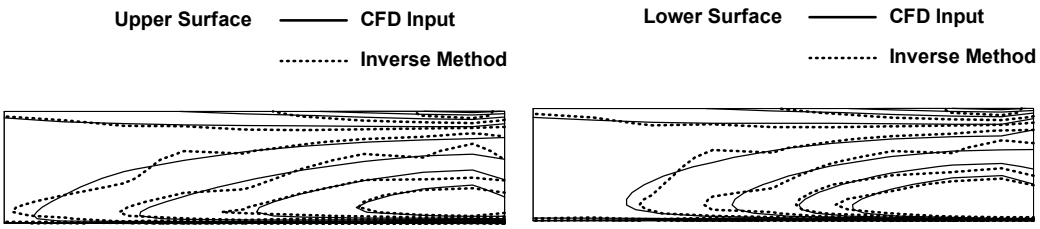


(a) (b)

**Figure 6.** The pressure contour of lower surface and upper surface

Figure 7 shows the pressure distributions of the four span locations, 0.94,0.8,0.64 and 0.4 respectively. The $\eta = 0.94$ represents the rotor tip position and $\eta = 0.4$ represents the rotor root position. The solid line is the pressure obtained by CFD simulation. The dashed line is the inverse method solution without aerodynamic constraint. The dotted line is the inverse method solution with aerodynamic constraint. It can be seen that approximate pressure distribution can be reconstructed by solving the inverse problem. There is a significant numerical oscillation when the aerodynamic constraint is not taken into account. As aerodynamic constraint is considered, a smoother solution can be obtained.

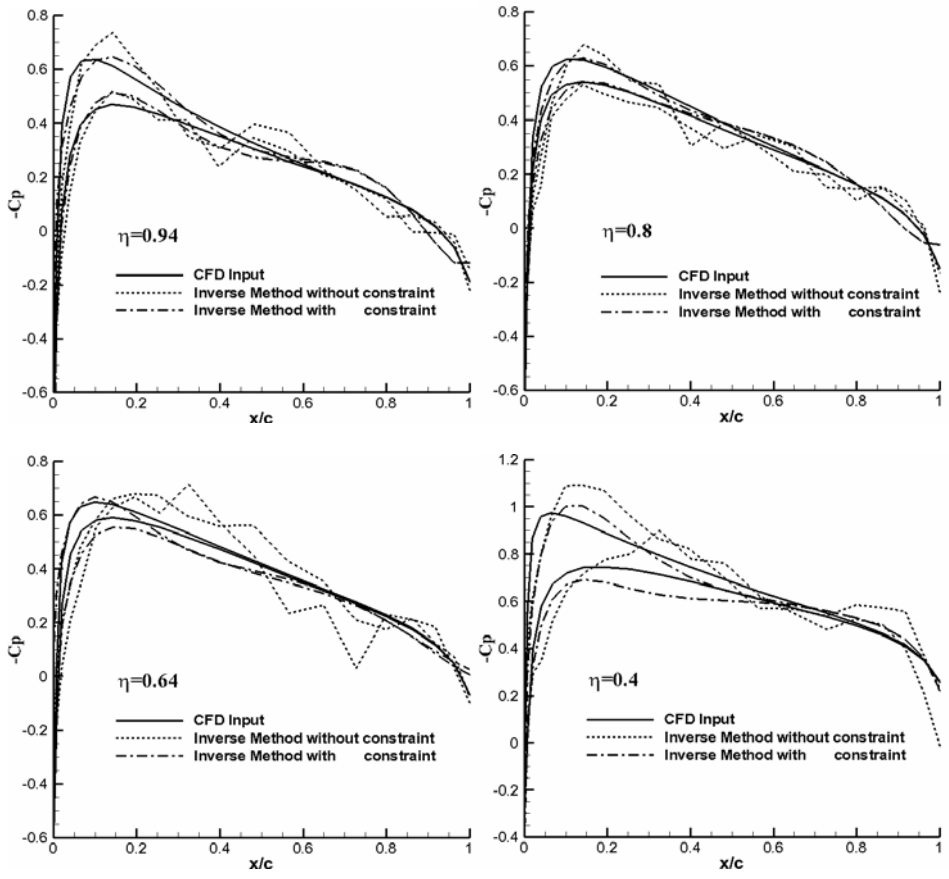


**Figure 7.** Comparison of Cp between inverse method solution and the CFD input data

*4.2. Inverse problem case with noise*

To simulate the measurement errors as in real physical cases, interference noise is added to exact sound signal. The interference noise includes wind tunnel background noise, measurement noise of microphones and et al.

Preprints (www.preprints.org) | NOT PEER-REVIEWED | Posted: 5 February 2018 doi:10.20944/preprints201802.0032.v1

$$[p]_m = [p]_d + e \tag{16}$$

where $[p]_m$ is the simulated sound pressure, $[p]_d$ is the exact sound pressure and $e$ is the interference noise, which has zero mean and covariance matrix $\sigma_g^2$ . The signal-to-noise ratio is defined as follows

$$\frac{S}{N} = \left[ \frac{1}{m} \frac{\|[p]_d\|^2}{\sigma_g^2} \right]^{1/2} \tag{17}$$

Figure 8 shows the pressure contour lines of the rotor surface with interference noise. It can be seen that under a certain signal-to-noise ratio, it is still possible to reconstruct a similar results. Although the contours are different, the trend distribution is the same basically. The result on the lower surface is better than the result on the upper surface.

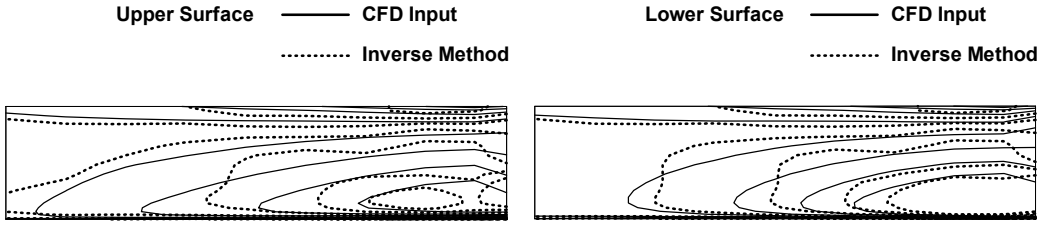


(a) (b)

**Figure 8.** The pressure contour of lower surface and upper surface

Figure 9 shows the reconstructed results considering interference noise, and the span locations and the legend are as same as in Figure 7. It can be seen that the reconstruction results will be worse when considering interference noise. When the aerodynamic constraint is not taken into account, the numerical oscillations decrease, but the pressure peaks shift back and the overall result deteriorates. When the aerodynamic constraint is taken into account, the reconstructed pressure peak position is more accurate, and the result is close to CFD Input.

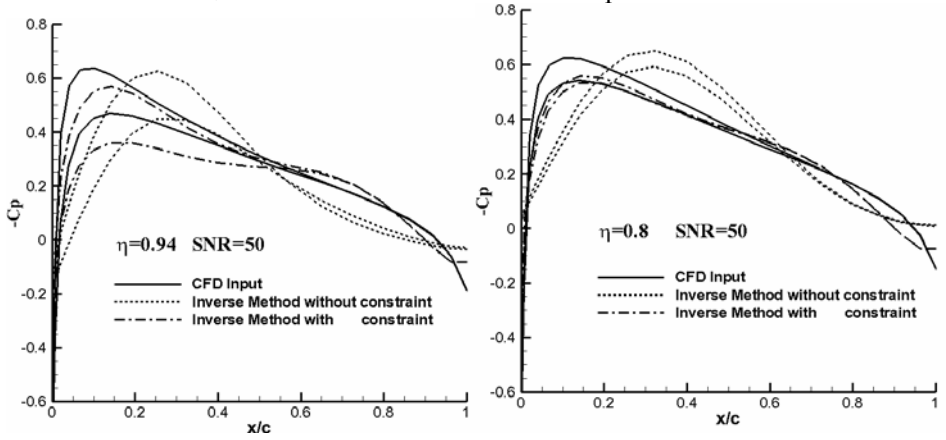

Preprints (www.preprints.org) | NOT PEER-REVIEWED | Posted: 5 February 2018 doi:10.20944/preprints201802.0032.v1

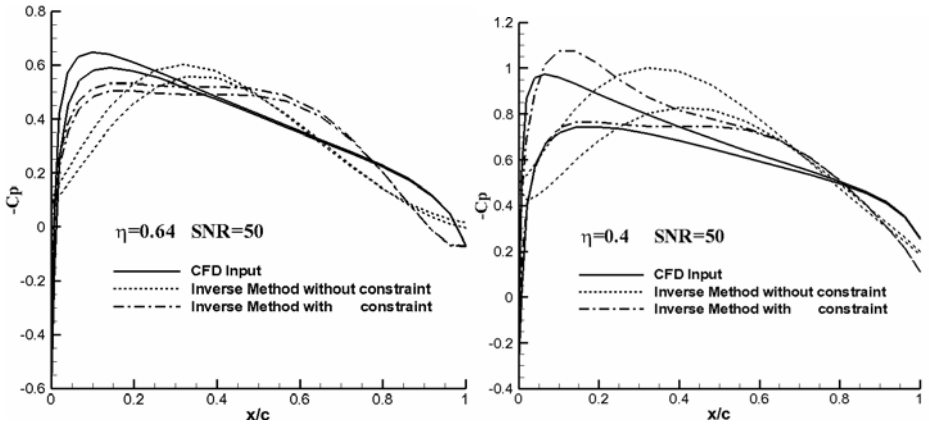


**Figure 9.** Comparison of Cp between inverse method solution and the CFD input data

## 5. Conclusions

Pressure reconstruction method is developed based on acoustic measurement. Singular value decomposition compiled with regulation method is applied to obtain the stable solution. The aerodynamic constraint is taken into accounted to ensure the numerical solution comply with the physics laws. ISL rotor model was performed to test the algorithm, the reconstructed pressure contour is reasonable and smooth. The pressure distribution of several different cross section positions are compared. The solutions of inverse method are very close to the input data. The influence of interference noise is also been considered, at low signal noise ratio condition, the closer results can also be obtained. It is shown that the aerodynamic constraints can eliminate non-physical oscillations and yield reasonably good results even at low signal noise ratio condition.

**Acknowledgments:** This work is supported by the National Science Foundation 51476005 and 91752204 of China.

**Author Contributions:** Xiaodong Li conceived, design the numerical simulations. Qinghe Zhao wrote the paper. All authors have reviewed and approved the final manuscript.

**Conflicts of Interest:** The authors declare no conflict of interest.

## References

1. Woan, C. J. ; Gregorek, G. M. The Exact Numerical Calculation of Propeller Noise, 1978, *AIAA* 78-1122
2. Boxwell, D. A.; Yu, Y. H.; Schmitz, F. H. Hovering Impulsive Noise. Some Measured and Calculated Results. *Vertica*, 1979, Vol.3
3. Caranonna, F. X.; Tung, C. Experimental and Analytical Studies of a Model Helicopter Rotor in Hover (1981)
4. Kuntz, M.; Lohmann, D.; Lieser, J. A.; PAHLKE, K. Comparison of Rotor Noise Predictions Obtained by lifting Surface Method and Euler Solutions Using Kirchhoff Equation, 16th *AIAA Aeroacoustic Conference*, 1995, June 12-15
5. Kuntz, M. Rotor Noise Prediction in Hover and Forward Flight Using Different Aeroacoustic Method, *AIAA*-96-1695
6. Li, X. D.; ZHOU, S. Spatial Transformation of the Discrete Sound Field from a Propeller, *AIAA Journal*, *Vol*,34, No 6, 1996, 1097-1102
7. Grace, S. P.; ATASSI, H. M. Inverse Aeroacoustic Problem for a Streamlined Body, Part 1:Basic Formulation, *AIAA Journal*, 1996,*Vol*.34, No.11, 2233-2240
8. Grace, S. P.; ATASSI, H. M. Inverse Aeroacoustic Problem for a Streamlined Body, Part 2:Basic Formulation, *AIAA Journal*, 1996, *Vol*.34, No.11, 2241-2246
9. Yoon. S. H.; Nelson, P. A. Reconstruction of Aeroacoustic Source Strength Distributions by Inverse Techniques, *AIAA*-98-2339

10. Wood, T. H.; Grace, S. M. Inverse Aeroacoustic Problem for a Rectangular Wing, *AIAA Journal*, 2000, *Vol.*38, No.2, 203-210
11. Yu, C.; Zhou, Z. F.; Zhuang, M. An Acoustic Intensity-Based Inverse Method for Sound Propagations in Uniform Flows, *AIAA paper* 2007-3563
12. Trabelsi, H.; Abid, M.; Taktak, M.; Fakhfakh, T.; HADDAR M. Reconstruction of the unsteady rotating forces of fan's blade from far-field sound pressure, *Applied Acoustic* (2014)
13. Zhang, X. Z.; Bi, C. X.; Zhang, Y. B.; XU, L. A time-domain inverse technique for the localization and quantification of rotating sound sources, *Mechanical Systems and Signal Processing* (2017)
14. Madoliat, R.; Nouri, N.; Rahrovi, A. Acoustic model order reduction for the lowest condition number in inverse method, *AIP Advances* (2017)
15. Tikhonov, A. N. Solution of incorrectly formulated problems and the regularization method, *Dokl. Akad. Nauk SSSR*, 1963, 151, pp. 501-504 *Soviet Math. Dokl.*, 4, 1035-1038
16. Tikhonov, A. N.; Arsenin, V. Y. Solutions of Ill-posed problems, Winston and Sons, Washington (1977)
17. Hansen, P. C. Analysis of Discrete ILL-Posed Problems By Means of The L-Curve, *SIAM Review*, 1992, Vol.34, No.4
18. Ffowcs Williams, J. E.; Hawkings, D.L. Sound Generated by Turbulence and Surface in Arbitrary Motion, Philosophical Transactions of the Royal Society of London, Vol. 264A, 1969, pp.321-342
19. Farassat, F.; Brown, T. J. A New Capability for Predicting Helicopter Rotor and Propeller Noise Including Flow and Motion, *NASA TM*-74037 (1977)
20. Farassat, F. Linear Acoustic Formulas for Calculation of Rotating Blade Noise, *AIAA Journal*, 1981, *Vol.*19, No.9, 1122-1130
21. Farassat, F. The Evolution of Methods for Noise Prediction of High Speed Rotors and Propellers in the time Domain, Recent Advances in Aeroacoustic, edited by A.Krothapalli and C.A.Smith, Springer-Verlag, New York, 129-147 (1986)
22. Gnemmi. P.; Haertig. J.; Jone, CH. Validation of the ROTAC code for the rotor noise prediction. 18th European Rotorcraft Forum, Avignon, France, 1992, September 15-18
23. Gnemmi. P.; Haertig. J.; Jone. CH.; ALBE, F. Measurements on the ISL rotor model. 15th International Congress on Instrumentation in Aerospace Simulation Facilities (ICIASF'93), Saint-Louis, France, 1993, September 20-23